Letter Vol. 44, No. 2 / 15 January 2019 / Optics Letters 431

Optics Letters

Generalized nonlinear Snell's law at $\chi^{(2)}$ modulated nonlinear metasurfaces: anomalous nonlinear refraction and reflection

Jing Zhang,[1,2] Xiaohui Zhao,[2,3] Yuanlin Zheng,[1,2] and Xianfeng Chen[1,2,*]

[1]State Key Laboratory of Advanced Optical Communication Systems and Networks, School of Physics and Astronomy, Shanghai Jiao Tong University, 800 Dongchuan Road, Shanghai 200240, China
[2]Key Laboratory for Laser Plasmas (Ministry of Education), Collaborative Innovation Center of IFSA (CICIFSA), Shanghai Jiao Tong University, 800 Dongchuan Road, Shanghai 200240, China
[3]Shanghai Institute of Laser Plasma, Shanghai 201800, China
*Corresponding author: xfchen@sjtu.edu.cn

Received 11 October 2018; revised 15 December 2018; accepted 18 December 2018; posted 19 December 2018 (Doc. ID 348065); published 15 January 2019

The generalized nonlinear Snell's law at the $\chi^{(2)}$ modulation surface is deduced from the universal model of $\chi^{(2)}$ processes in nonlinear photonic crystals (NPhCs). Based on the generalized nonlinear Snell's law, the anomalous refraction and reflection geometries are predicted and observed at crystal's inner boundary on nonlinear metasurfaces formed by one-dimensional NPhCs. The emitted second harmonic is observed, which obeys the law and appears to turn into multiple orders compared to that in a bulk crystal. Furthermore, the analysis shows a potential way to achieve nonlinear over-reflection by using submicron periodic $\chi^{(2)}$ modulation in metasurfaces.

https://doi.org/10.1364/OL.44.000431

The Snell's law is a fundamental optical principle describing the behavior of an optical wave passing through the interface between two media with different refractive indices [1]. By introducing linear phase shifts artificially, the linear interfaces become metasurfaces [2], for which the Snell's law has been generalized to describe the corresponding optical behavior. Metasurfaces have attracted considerable interest in recent years and have been employed to demonstrate extraordinary phenomena, such as negative refraction [3,4], perfect absorption [5,6], and polarization modulation [7]. Since high-intensity coherent light sources have arisen, nonlinear optical effects have been increasingly investigated [8]. When an optical wave passes the interface with different second-order susceptibilities at both sides, the trajectories of the emitted harmonic waves obey a similar rule to its linear counterpart, called the nonlinear Snell's law [9], which is deduced by solving Maxwell's equations at the boundary conditions [10]. Likewise, how harmonic waves behave at nonlinear modulated interface, which shall be called nonlinear metasurfaces [11–14], is attractive with an important aspect. Hence, many more characteristics of harmonic waves are to be investigated, which allows for further practical applications, such as harmonic conversion [15,16], nondestructive diagnostics [17], and ultrashort pulse characterization [18,19]. Besides, with the modulation of $\chi^{(2)}$ in nonlinear metasurfaces, where harmonic generation becomes more varied [20], the changes to the nonlinear Snell's law under $\chi^{(2)}$ modulation need to be revised and generalized.

In this research, the nonlinear effects at one-dimensional (1D) NPhC boundaries, which actually form nonlinear metasurfaces, are demonstrated using the universal model of $\chi^{(2)}$ processes [21], both theoretically and experimentally. Modulated by a periodic $\chi^{(2)}$ structure, the nonlinear Snell's law is generalized turning into a form that is similar to that in linear metasurfaces, achieving anomalous refraction and reflection with multiple-order second harmonics (SHs). Accordingly, a periodically poled lithium niobate (PPLN) crystal sample is employed in the experiment to demonstrate the characteristics of multiple-order SHs and verify the revised law, accompanied with a control group of a bulk lithium niobate (LN) sample. Furthermore, a potential method utilizing submicron periodic $\chi^{(2)}$ modulated metasurfaces to realize nonlinear over-reflection is proposed from the generalized nonlinear Snell's law.

As for the refraction and reflection on boundaries of nonlinear crystals, the trajectories of the reflected and refracted waves follow the nonlinear Snell's law [9], as shown in Fig. 1(a):

$$n(\omega_1)\sin\alpha = n(\omega_2)\sin\theta_r = n_0(\omega_2)\sin\theta_t, \qquad (1)$$

where α, θ_r, and θ_t are the angles of incidence, reflection, and transmission, respectively. In addition, n is refractive index of crystals, n_0 is refractive index of space, ω is the wave's angular frequency, and subscripts 1 and 2 denote fundamental wave (FW) and SH, respectively. The corresponding phase-matching condition in reciprocal space is illustrated in Fig. 1(b), where k_1, k_2, and k_{np} denote the wave vector of FW, SH and the nonlinear polarization wave, respectively. It is a similar form to that of linear Snell's law shown in Fig. 1(c).

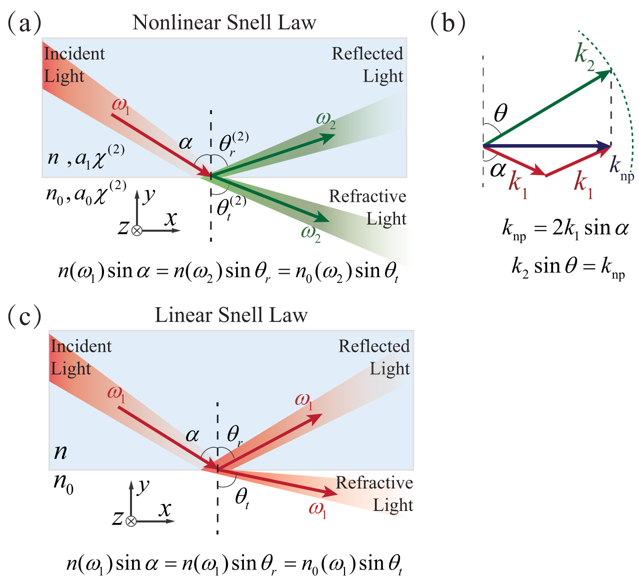

Fig. 1. (a) Nonlinear Snell's law of refraction and reflection on the boundary of nonlinear crystals; (b) taking the reflection, for example, spontaneously longitudinal partial space phase-matching SH satisfies the law; (c) linear Snell's law of refraction and reflection on the boundary of linear crystals.

As for $\chi^{(2)}$ modulated nonlinear metasurfaces, the $\chi^{(2)}$ process becomes more complicated with the compensation in reciprocal vectors in lattices where the SH that obeys the nonlinear Snell's law becomes multiple orders, as shown in Fig. 2(a). Since the nonlinear metasurfaces operated here are formed by NPhCs, we start the analysis with 1D NPhCs for simplicity to derive the corresponding nonlinear Snell's law. We assume that FW, a Gaussian beam with a waist radius of w, is incident into a 1D NPhC at an angle of α to the x axis and generates SHs, which is expressed as [21]

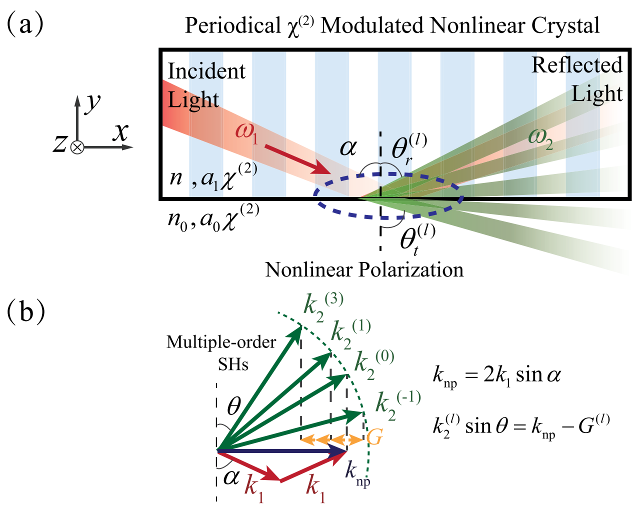

Fig. 2. (a) FW at oblique incidence to the crystal inner boundary in NPhCs; the stimulated sum-frequency nonlinear polarization along the boundary generates SHs with anomalous multiple orders. (b) Taking the reflections, for example, it is the compensation of reciprocal vectors in NPhCs that turn SH that obeys the law into multiple orders.

$$\begin{cases} I_2 = \frac{w^4\pi^2}{4}\beta_2^2 I_1^2 x^2 \left| \sum_l C_l \,\mathrm{sinc}\left[\left(k_x - k_{\mathrm{np}} + \frac{2l\pi}{\Lambda}\right)\frac{x}{2}\right]\right|^2 F(k_y) e^{-\frac{w^2}{4}k_z^2} \\ F(k_y) = \frac{\pi}{4}\left|\frac{1}{\sqrt{2}}(a_1 + a_0)e^{-\frac{w^2}{8}k_y^2} + i(a_1 - a_0)wD\sqrt{\frac{w^2k_y^2}{8}}\right|^2 \end{cases}, \quad (2)$$

where I denotes the intensity; β_2 is a coefficient related with k_2; Λ denotes the lattice period; and k_x, k_y, and k_z are the x-component, y-component, and z-component of k_2, respectively. In addition, function $D(x)$ denotes Dawson function. Besides, a_1 and a_0 are moduli of $\chi^{(2)}$ of the crystal and outer space, respectively. When $a_1 - a_0 = 0$, it means that $\chi^{(2)}$ across the interface is homogeneous, and SH will mainly focus on the direction where $k_y = 0$. When $a_1 - a_0 \neq 0$, SH will emit at the Cherenkov angle with an intensity depending on the value of $D(x)$ and in proportional to $|a_1 - a_0|^2$. Consequently, emission conditions of multiple-order SHs can be derived as $k_2^{(l)}$ sin $\theta = k_{\mathrm{np}} - G^{(l)}$ with order l, where $G^{(l)} = lG_0 = l \cdot \frac{2\pi}{\Lambda}$, and G_0 is the unit reciprocal vector in the x direction, and different l's correspond to different orders.

Figure 2(b) shows the phase-matching condition in reciprocal space. The non-zero even orders are omitted. It is because the factor C_l in Eq. (2) can be derived as $C_l = \mathrm{sinc}\frac{l\pi}{2}$ (l denoting the ordinal of Fourier series) due to 1:1 duty cycle. When l takes the value of non-zero even numbers, $C_l = 0$; then $I_2 = 0$. Consequently, non-zero even-order SHs do not exist.

As for refractive indices at both sides of the interface, whether the trajectory of the SH is reflective or refractive depends on the specific value of n. When n of crystal is similar to n_0 of the outer space, the refractive SHs are emitted; when n is much larger than n_0, SHs shall get totally reflected at the inner side of the interface, i.e., the crystal boundary. Thus, the emission condition of the SH wave can be rewritten as

$$n(\omega_1)\sin\alpha + \frac{\lambda_1}{2\pi}\left[\frac{G^{(-l)}}{2}\right] = n(\omega_2)\sin\theta_r^{(l)} = n_0(\omega_2)\sin\theta_t^{(l)}. \quad (3)$$

This is the generalized Snell's law for $\chi^{(2)}$ processes in nonlinear metasurfaces. It can be compared with the generalized Snell's law for gradient metasurfaces, i.e., $n_1 \sin\alpha + \frac{\lambda_0}{2\pi}\frac{d\Phi}{dx} = n_1 \sin\theta_r = n_2 \sin\theta_t$ [2]. The resemblance between these two equations shows a potential way to achieve similar modulations to those of metasurfaces in nonlinear optical materials. To this extent, the $\chi^{(2)}$ lattice structures formed by 1D NPhCs can be called nonlinear metasurfaces. Hence, Eq. (3) is the generalized nonlinear Snell's law describing the anomalous $\chi^{(2)}$ refraction and reflection geometry behaviors.

Equation (3) indicates that the refractive and reflective trajectories possess similar behaviors, and there is only a slight difference caused by n. Because the refraction tends to disappear due to the total reflection in most cases, we demonstrate the behavior of the reflection to analyze the characteristics of the law. The emission angle of the l-order reflective SHs along the x-axis is deduced as

$$\theta^{(l)} = \arcsin\frac{n(\omega_1)\sin\alpha + \frac{\lambda_1}{2\pi}\left[\frac{G^{(-l)}}{2}\right]}{n(\omega_2)} = \arcsin\frac{2k_1 \sin\alpha - lG_0}{k_2}. \quad (4)$$

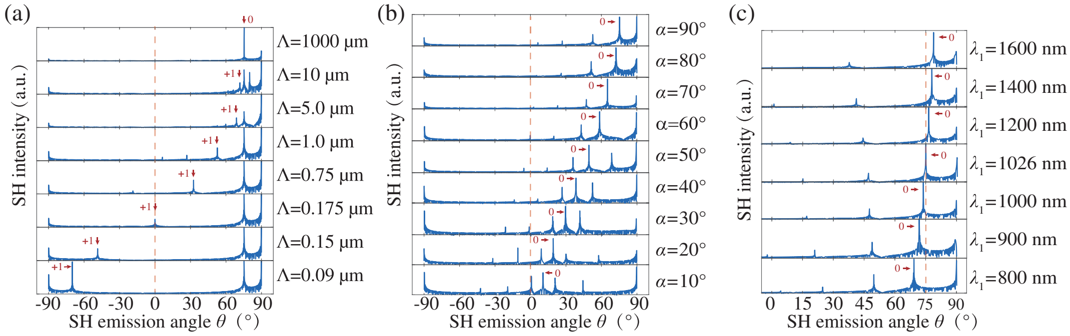

Fig. 3. Simulation results of emitted SH in different incident angles, lattice periods, and FW wavelengths. (a) 800 nm FW wavelength and incident angle of 90° staying constant; the multiple-order SH emission angles vary with the lattice period. (b) 800 nm FW wavelength with a lattice $\chi^{(2)}$ period of 1 μm staying constant; the multiple-order SH emission angles vary with the incident angle. (c) FW incident angle of 75° with the lattice $\chi^{(2)}$ period of 1 μm staying constant; the multiple-order SH emission angles vary with FW wavelength.

Together with Eq. (2), the simulation results can be illustrated as shown in Fig. 3. Taking PPLN as an example, when the FW wavelength and incident angle stay constant, as shown in Fig. 3(a), the position of 0-order SH remain unchanged, whereas the angles of positive orders increase as the lattice period shrinks. When the FW incident angle alters, as shown in Fig. 3(b), there is an overall movement of SHs centered on 0 order. Besides, as the incident angle decreases, negative order SHs show up successively. The emission angle of the 0-order SH altered with the incident angle on the whole, while it is also was slightly influenced by the incident wavelength, as shown in Fig. 3(c). As the wavelength decreases, the 0-order SH moves from the inner side of the reflective FW to the outer side. Moreover, it is worth noting that a few orders of SHs in Figs. 3(a) and 3(b) are possible to exceed the interface normal realizing over-reflection, only in the condition of a very small lattice period which is under submicron size. However, it is quite a challenge now to achieve such artificial fabrication in this small scale [22–26].

Taking the *oo-e* type SH at the FW of 1064 nm as an example, two z-cut LN (z-axis is the crystal's optical axis) samples in the size of $3 \times 3 \times 1.0$ mm ($x \times y \times z$) are employed. The first sample is a single-domain bulk 5 mol% $MgO:LiNbO_3$ crystal, while the second one is periodically poled with a period of 13.9-m, and the domain wall is along the ya€ z plane. The fundamental beam was derived from a mode-locked Nd:YAG nanosecond laser which generated 4 ns pulses centered at a wavelength of 1064 nm at a repetition rate of 20 Hz. A O-polarized FW is focused into the sample ($f = 10$ cm) along the x-axis after being modulated by a Glan–Taylor polarizer. Then we place the sample on a rotation stage at room temperature (20°C), as shown in Fig. 4(a). Accordingly, the coefficients are determined as $n_0 = 1$, $a_1 = 1$, and $a_0 = 0$. Since the refractive index in the crystal is much larger than that in the air, total reflection happens at the inner surface of the sample, and it gets reflected out from the other side.

The experimental pictures are shown in Figs. 4(b) and 4(c). From the comparison, SH modulated by a nonlinear metasurface which is formed by the PPLN inner boundary turns into anomalous multiple orders, whereas the 0-order normal SH maintains the same trajectory.

The distance of FW and SH on the screen was measured to calculate the emission angle according to geometrical relationship. Hence, an incidence-emission angle diagram is calculated and displayed with the organized experimental data in Fig. 5. Obviously, the SH spots that obey the law are much weaker than spots A and B, which are due to the partial phase-matching $\chi^{(2)}$ processes. Secondly, with the backward G's compensation, positive-order SHs emit at smaller angles than the 0-order one. While with the forward G's compensation, negative-order SHs emit at larger angles than the 0-order one and are cut off until the angle close to 90°. As the incident angle decreasing, the 0-order, −1-order, and −3-order appear successively. In addition, there are generally only several lower orders that can emit because of the coefficient C_l in Eq. (2). Moreover, it also can be seen experimentally that non-zero even orders do not exist due to the 1:1 duty cycle.

So far, we have obtained the generalized nonlinear Snell's law for 1D nonlinear metasurfaces, which has form that resembles that of metasurfaces, showing a potential way to achieve similar modulations. Besides, providing more radiation patterns

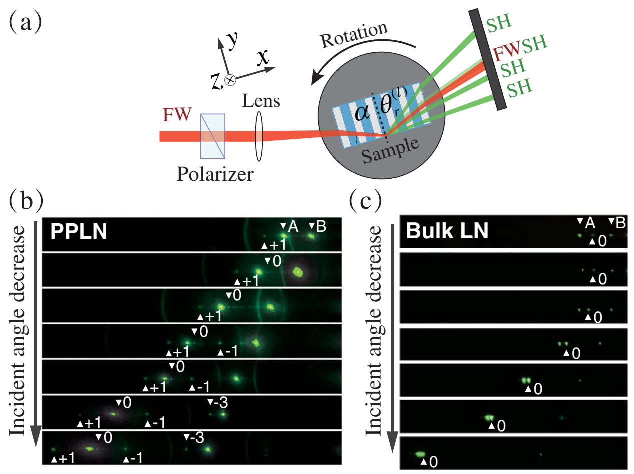

Fig. 4. (a) Diagram of the experimental setup. (b) Experimental group with the PPLN crystal, with the incident FW angle decreasing; multiple-order SHs that obey the law are generated. Besides, point A is the SH collinear with the reflected FW, and point B is the SH along the crystal boundary. The numbers denote the corresponding SH order. (c) Control group with a bulk crystal, with the incident FW angle decreasing; only a single-order SH is generated.

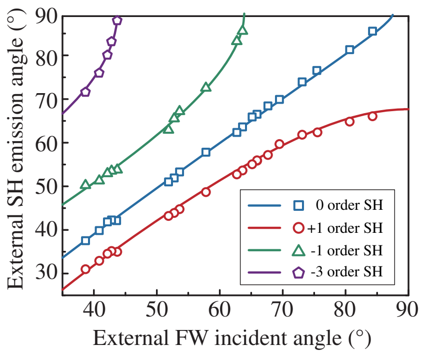

Fig. 5. Theoretical results of SH emission angles and the corresponding experimental data of different orders of SHs in the PPLN sample; the measurement error is within ±1°.

compared with bulk crystal surfaces, it presents a expecting possibility of plentiful radiation patterns in other $\chi^{(2)}$ structures, such as aperiodic, quasi-periodic, random, chirp, two-dimensional, and other desirable patterns. Further, making appropriate artificial structures on NPhC surfaces would form different types of nonlinear metasurfaces, allowing more efficient controls in harmonic generation.

In summary, we verified that the periodic $\chi^{(2)}$ structures on a crystal surface form a nonlinear metasurface to modulate the trajectories of SHs, realizing anomalous multiple-order SHs, compared to the conventional reflection and refraction geometries at a crystal boundary. The generalized nonlinear Snell's law is derived to describe the reflection and refraction at a $\chi^{(2)}$ modulated nonlinear metasurface. Moreover, it indicates a potential method to realize nonlinear over-reflection by utilizing submicron periodic $\chi^{(2)}$ modulated metasurfaces.

Funding. National Key R&D Program of China (2017YFA0303700); National Natural Science Foundation of China (NSFC) (11734011); The Foundation for Development of Science and Technology of Shanghai (17JC1400400).

REFERENCES

1. M. Born and E. Wolf, *Principles of Optics: Electromagnetic Theory of Propagation, Interference and Diffraction of Light* (Elsevier, 2013).
2. N. Yu, P. Genevet, M. A. Kats, F. Aieta, J.-P. Tetienne, F. Capasso, and Z. Gaburro, Science **334**, 333 (2011).
3. S. Sun, K.-Y. Yang, C.-M. Wang, T.-K. Juan, W. T. Chen, C. Y. Liao, Q. He, S. Xiao, W.-T. Kung, G.-Y. Guo, L. Zhou, and D. P. Tsai, Nano Lett. **12**, 6223 (2012).
4. A. Pors, O. Albrektsen, I. P. Radko, and S. I. Bozhevolnyi, Sci. Rep. **3**, 2155 (2013).
5. N. Liu, M. Mesch, T. Weiss, M. Hentschel, and H. Giessen, Nano Lett. **10**, 2342 (2010).
6. C. M. Watts, X. Liu, and W. J. Padilla, Adv. Mater. **24**, OP98 (2012).
7. J. Hao, Y. Yuan, L. Ran, T. Jiang, J. A. Kong, C. Chan, and L. Zhou, Phys. Rev. Lett. **99**, 063908 (2007).
8. R. W. Boyd, *Nonlinear Optics* (Elsevier, 2003).
9. X. Zhao, Y. Zheng, H. Ren, N. An, X. Deng, and X. Chen, Phys. Rev. A **95**, 043841 (2017).
10. N. Bloembergen and P. Pershan, Phys. Rev. **128**, 606 (1962).
11. A. E. Minovich, A. E. Miroshnichenko, A. Y. Bykov, T. V. Murzina, D. N. Neshev, and Y. S. Kivshar, Laser Photonics Rev. **9**, 195 (2015).
12. W. Ye, F. Zeuner, X. Li, B. Reineke, S. He, C.-W. Qiu, J. Liu, Y. Wang, S. Zhang, and T. Zentgraf, Nat. Commun. **7**, 11930 (2016).
13. N. Nookala, J. Lee, M. Tymchenko, J. S. Gomez-Diaz, F. Demmerle, G. Boehm, K. Lai, G. Shvets, M.-C. Amann, A. Alu, and M. Belkin, Optica **3**, 283 (2016).
14. F. Walter, G. Li, C. Meier, S. Zhang, and T. Zentgraf, Nano Lett. **17**, 3171 (2017).
15. C. Chen, J. Lu, Y. Liu, X. Hu, L. Zhao, Y. Zhang, G. Zhao, Y. Yuan, and S. Zhu, Opt. Lett. **36**, 1227 (2011).
16. Y. Sheng, W. Wang, R. Shiloh, V. Roppo, Y. Kong, A. Arie, and W. Krolikowski, Appl. Phys. Lett. **98**, 241114 (2011).
17. X. Deng and X. Chen, Opt. Express **18**, 15597 (2010).
18. S. Holmgren, C. Canalias, and V. Pasiskevicius, Opt. Lett. **32**, 1545 (2007).
19. A. Aleksandrovsky, A. Vyunishev, A. Zaitsev, A. Ikonnikov, and G. Pospelov, Appl. Phys. Lett. **98**, 061104 (2011).
20. X. Zhao, Y. Zheng, N. An, X. Deng, H. Ren, and X. Chen, Opt. Express **25**, 13897 (2017).
21. J. Zhang, X. Zhao, Y. Zheng, H. Li, and X. Chen, Opt. Express **26**, 15675 (2018).
22. V. Y. Shur, P. Zelenovskiy, M. Nebogatikov, D. Alikin, M. Sarmanova, A. Ievlev, E. Mingaliev, and D. Kuznetsov, J. Appl. Phys. **110**, 052013 (2011).
23. A. Gruverman and A. Kholkin, Rep. Prog. Phys. **69**, 2443 (2005).
24. X. Chen, P. Karpinski, V. Shvedov, K. Koynov, B. Wang, J. Trull, C. Cojocaru, W. Krolikowski, and Y. Sheng, Appl. Phys. Lett. **107**, 141102 (2015).
25. V. Y. Shur, A. Akhmatkhanov, and I. Baturin, Appl. Phys. Rev. **2**, 040604 (2015).
26. X. Chen, P. Karpinski, V. Shvedov, A. Boes, A. Mitchell, W. Krolikowski, and Y. Sheng, Opt. Lett. **41**, 2410 (2016).